NO_x Reduction by Air-Side Versus Fuel-Side Dilution in Hydrogen Diffusion Flame Combustors

Nathan T. Weiland
National Energy Technology Laboratory,
Pittsburgh, PA 15236-0940;
Department of Mechanical and Aerospace Engineering,
West Virginia University,
Morgantown, WV 26506-6106
e-mail: nathan.weiland@mail.wvu.edu

Peter A. Strakey
National Energy Technology Laboratory,
Morgantown, WV 26507-0880

Lean-direct-injection (LDI) combustion is being considered at the National Energy Technology Laboratory as a means to attain low NO_x emissions in a high-hydrogen gas turbine combustor. Integrated gasification combined cycle (IGCC) plant designs can create a high-hydrogen fuel using a water-gas shift reactor and subsequent CO_2 separation. The IGCC's air separation unit produces a volume of N_2 roughly equivalent to the volume of H_2 in the gasifier product stream, which can be used to help reduce peak flame temperatures and NO_x in the diffusion flame combustor. Placement of this diluent in either the air or fuel streams is a matter of practical importance, and it has not been studied to date for LDI combustion. The current work discusses how diluent placement affects diffusion flame temperatures, residence times, and stability limits, and their resulting effects on NO_x emissions. From a peak flame temperature perspective, greater NO_x reduction should be attainable with fuel dilution rather than air or independent dilution in any diffusion flame combustor with excess combustion air, due to the complete utilization of the diluent as a heat sink at the flame front, although the importance of this mechanism is shown to diminish as flow conditions approach stoichiometric proportions. For simple LDI combustor designs, residence time scaling relationships yield a lower NO_x production potential for fuel-side dilution due to its smaller flame size, whereas air dilution yields a larger air entrainment requirement and a subsequently larger flame, with longer residence times and higher thermal NO_x generation. For more complex staged-air LDI combustor designs, the dilution of the primary combustion air at fuel-rich conditions can result in the full utilization of the diluent for reducing the peak flame temperature, while also controlling flame volume and residence time for NO_x reduction purposes. However, differential diffusion of hydrogen out of a diluted hydrogen/nitrogen fuel jet can create regions of higher hydrogen content in the immediate vicinity of the fuel injection point than can be attained with the dilution of the air stream, leading to increased flame stability. By this mechanism, fuel-side dilution extends the operating envelope to areas with higher velocities in the experimental configurations tested, where faster mixing rates further reduce flame residence times and NO_x emissions. Strategies for accurate computational modeling of LDI combustors' stability characteristics are also discussed.
[DOI: 10.1115/1.4000268]

1 Introduction

Following the deregulation of the electric power industry, the integrated gasification combined cycle (IGCC) power plant has become increasingly interesting to power producers, due to its increased efficiency and reduced footprint, capital cost, and emission controls relative to conventional coal-fired power plants. In addition, reduction in CO_2 emissions can be accommodated in the IGCC plant design by using a water-gas shift reactor to convert steam and the CO in the gasified coal (syngas) to hydrogen and CO_2, which is separated and sequestered, leaving a relatively high-purity hydrogen fuel for combustion in the gas turbine. Pending future regulation of CO_2 emissions, an increase in the number of likely future IGCC installations with carbon capture and sequestration capabilities presents an opportunity to redesign the gas turbine combustor to more efficiently utilize high-hydrogen fuels.

The mode of combustion currently used for syngas and high-hydrogen fuels in gas turbine engines is dominated by swirl-based diffusion flames [1–6]. In comparison to premixed flames, these are much more tolerant of variations in the fuel content, and are also immune to the damaging effects of flashback and autoignition that plague high-hydrogen premixed flames due to hydrogen's high flame speed. However, stoichiometric conditions at the flame front result in high peak flame temperatures and hence high levels of NO_x production in diffusion flames. In addition, there has been little optimization of the traditional swirl-based combustor design to accommodate diffusion flame combustion of high-hydrogen fuels.

Much work has been done in recent years on lean-direct-injection (LDI) burners [7–14], where fuel and excess air are introduced separately into the combustor and are rapidly mixed in an attempt to approach lean premixed flame conditions. These combustors avoid the flashback issues associated with true premixed combustion systems, while producing NO_x emissions at levels below traditional swirl-based combustors, but still somewhat higher than premixed combustors. NO_x emission reductions in LDI combustors are achieved through distributed injection schemes, utilizing many small flames to reduce flame residence times. This is an improvement over traditional swirl-based com-

Contributed by the International Gas Turbine Institute (IGTI) of ASME for publication in the JOURNAL OF ENGINEERING FOR GAS TURBINES AND POWER. Manuscript received May 1, 2009; final manuscript received May 21, 2009; published online April 14, 2010. Editor: Dilip R. Ballal.

bustors that utilize large flames and longer residence times to improve CO burnout, a feature not required for high-hydrogen combustion.

LDI burners can be further subdivided into swirl-based [7–11] and jet-based injection schemes [12–14]. The swirl-based designs originally developed for liquid-fuelled aero-engines [8,9] have been recently modified to burn hydrogen fuel [10] and hold some promise for reducing NO_x emissions, though they are prone to flame anchoring issues at elevated pressures [11]. Flame anchoring too close to the injection point can overheat and damage the injector, which has been a problem for some jet-based LDI combustors [13].

While LDI combustors are still in the research stages for the combustion of high-hydrogen fuels, traditional swirl-based diffusion flame combustors have already been used in fielded turbines burning syngas [3,6,15]. These combustors have been able to achieve a low of 12–15 ppm NO_x with nitrogen dilution [15], though the addition of steam to the combustor is also used to reduce the combustion temperature and hence the NO_x production [16,17]. While frequently used, steam is not an ideal combustion diluent, as it increases the water consumption of the plant. Furthermore, the energy used to vaporize the water to form steam is not recovered in the power-producing turbine section, and steam addition increases the heat transfer to the turbine blades, thereby decreasing their effective lifespan. In an oxygen-blown IGCC plant, however, the air separation unit produces a nitrogen byproduct that can be used as a diluent in the combustion chamber, avoiding many of the issues associated with the steam dilution of the combustor [16]. In an air-blown IGCC, nitrogen from the air supplied to the gasification process is contained in the syngas, essentially diluting the fuel stream in such a combustor.

It is likely that substantial reductions in NO_x emissions can be realized by combining the dilution approach of traditional swirl-based combustors with the low residence times of LDI-style injectors. Utilization of a combustor diluent has not been studied for high-hydrogen fuelled LDI combustion systems to date with the exception of Ref. [14], which utilizes a 65% hydrogen and 35% nitrogen base fuel mixture. However, this study does not consider alternative dilution levels or arrangements, such as premixing the diluent with the combustion air or injecting the diluent separately into the combustor.

Studies of dilution placement in traditional swirl-based combustors have concluded that there is little difference between fuel or air dilution from a NO_x emission perspective [5,18], though this is largely an artifact of the near-stoichiometric conditions in the primary combustion zone in such combustors. One notable exception to these studies concluded that fuel-side dilution reduced NO_x more than air-side dilution in a model gas turbine combustor operating on methane, though the stoichiometry employed in these experiments is unknown [19].

Typically, diluent has been added to the combustion air stream to date, often to minimize the amount of redesign required to accommodate a high-hydrogen fuel in existing diffusion flame combustors. Due to its low energy content per unit volume, the diluent has typically not been added to the fuel as this would increase the required fuel flow rate, in some cases to eight times that in a higher energy density natural gas combustor, resulting in fuel manifold sizing problems [17]. In industrial diffusion flame combustion configurations, Feese and Turns [20] investigated the placement of a nitrogen diluent in either the methane or air streams, and concluded that the effects of dilution placement on flame residence time is of great importance to the overall NO_x emissions of the combustor.

Accordingly, the following study investigates the effect of nitrogen diluent placement on NO_x emissions of LDI-style hydrogen flames in a laboratory setting, including its effects on flame temperature, flame residence time, and static flame stability. In particular, this report targets simple turbulent diffusion flame designs, where swirl is imparted neither to the fuel nor air streams as they enter the combustion chamber, although some aspects of diluent placement with respect to swirl-based designs are addressed below, where applicable.

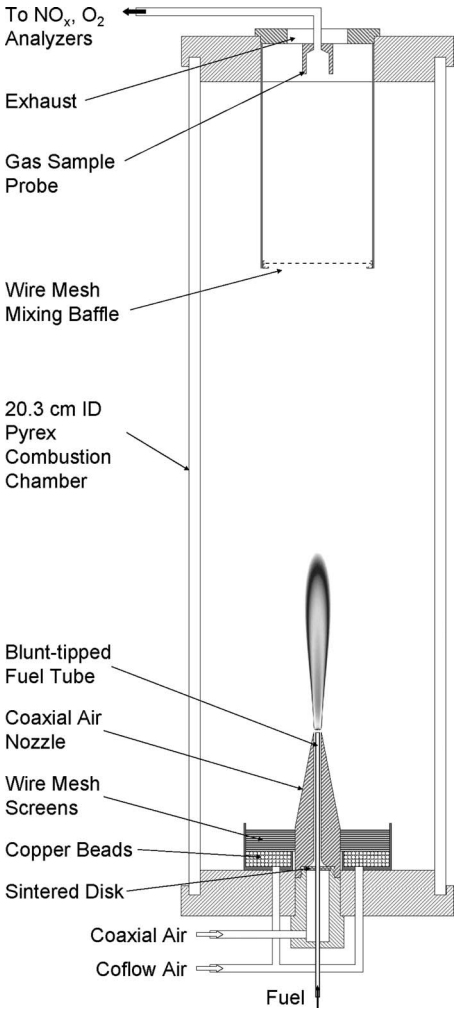

Fig. 1 Dilute diffusion flame combustor

2 Experimental Setup

The atmospheric pressure combustor used in the experimental portion of this study is shown in Fig. 1. The fuel tube has inside and outside diameters of d_F=1.45 mm and $d_{F,o}$=3.18 mm, respectively, and is positioned concentrically within interchangeable coaxial air nozzles of d_A=5.00 mm and 6.35 mm inside diameter. Additional air can be supplied as low-velocity coflow air to enable the effects of coaxial air velocity and global equivalence ratio to be studied separately in the combustor. High purity hydrogen, nitrogen, and air are metered separately to the combustor using independent mass flow controllers, while the nitrogen is supplied to either the hydrogen or coaxial air lines well upstream of the combustor to ensure full premixing of the diluent with its carrier stream.

At the top of the combustor, three wire mesh screens, suspended from the exhaust cap, are used to mix the combustion products in advance of the gas sampling, and they have been shown to eliminate sample profile effects without affecting the flame in the current set of experiments. A gas sample is drawn through a heated sample line to an NO_2 to NO converter, then through a gas cooler and a desiccant trap to remove the water vapor. The gas is then analyzed at steady state conditions by Rose-

mount chemiluminescent and paramagnetic detectors to measure the NO_x and oxygen content in the dry combustion products, respectively.

The measured NO_x is converted to a corrected NO_x using the measured product gas O_2 mole fraction and the following formula:

$$\chi_{NO_x,corr} = \chi_{NO_x,meas}\left(\frac{0.2095 - 0.15}{0.2095 - \chi_{O_2,meas}}\right)\left(1 + \frac{\frac{1}{2}(0.2095)}{1 - 0.2095}D\right) = 6.6 \times EINO_x \quad (1)$$

where D is the number of moles of nitrogen diluent per mole of hydrogen, and $EINO_x$ is the emission index in units (g NO_2/kg H_2). The first part of Eq. (1) is the standard correction to 15% O_2 in the combustion products [21], while the last term in parentheses accounts for the diluent effect of nitrogen on the corrected NO_x measurement, such that the same corrected NO_x results if the diluent nitrogen is replaced by the same number of moles of air to yield 15% O_2 in the dry combustion products. Equation (1) can be derived from the more general expression of ElKady et al. [22] as a special case for hydrogen combustion, though the result is greatly simplified if the quantity D is known, as it is in this work.

Computations of adiabatic flame temperatures were performed with the GASEQ program [23]. Computational fluid dynamic (CFD) modeling of the diluted coaxial air flames was done with FLUENT'S code, using a Reynolds stress model coupled with an eddy dissipation concept (EDC) model [24] and the H_2/O_2 chemical mechanism of Li et al. [25].

3 Results and Discussion

Simplified scaling analyses of thermal NO_x in a simple hydrogen turbulent jet flame predict that $EINO_x$ scales with flame residence time and the Damköhler number as [26]

$$EINO_x \propto t_{res}\ \mathrm{Da}^{-1/2}\frac{d[\mathrm{NO}]}{dt} \quad (2)$$

The flame temperature primarily affects NO_x production via the thermal NO production rate [27]

$$\frac{d[\mathrm{NO}]}{dt} \propto [\mathrm{O}][\mathrm{N_2}]e^{-38{,}370/T} \quad (3)$$

in which [O] and [N_2] are the concentrations of O-atoms and N_2 molecules, respectively, and T is the flame temperature in Kelvin. The residence time for a jet flame can be determined from the flame volume, which is proportional to the flame length cubed L_f^3, divided by the volume flow rate of fuel leaving the jet exit $U_F d_F^2$ [26]. Equations (2) and (3) form the basis for determining the effects of the dilution placement on NO_x through temperature and residence time effects, which will be considered individually in Secs. 3.1 and 3.2 for a simple jet configuration. Following this, more realistic LDI-type injection schemes are studied from an idealized coaxial jet configuration, where the effects of static flame stability and operating regimes on NO_x emissions can be determined.

3.1 Dilute Flame Temperatures. Calculated adiabatic flame temperatures for different types of flames and dilution scenarios are presented as a function of the overall combustor equivalence ratio in Fig. 2. For each level of nitrogen diluent available, premixed flame temperatures also represent fully mixed adiabatic combustor exit/turbine inlet temperatures for both premixed and nonpremixed combustor types. Peak diffusion flame temperatures, which control thermal NO_x formation, are also shown for air- and fuel-side nitrogen dilutions.

To illustrate the effects of the dilution placement on peak flame temperatures, consider the operation of the combustor at a global

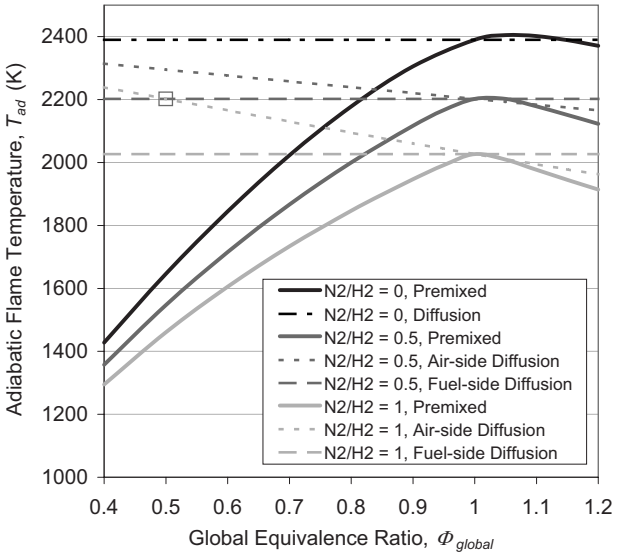

Fig. 2 Adiabatic flame temperatures for premixed and diffusion flames with varying N_2/H_2 dilution ratios

equivalence ratio of $\Phi_{global}=0.5$, where twice as much air is present than is needed for complete combustion. The dilution of the air stream at this equivalence ratio will result in half of the diluent arriving at the flame front, where the fuel and air meet in stoichiometric proportions. For air-side dilution with one mole of nitrogen per mole of hydrogen (the dotted light gray line in Fig. 2), this yields an equivalent adiabatic flame temperature to fuel-side dilution for $N_2/H_2=0.5$ (marked by the square in Fig. 2). By comparison, all of the diluent must pass through the flame front if it is added to the fuel stream, thereby reducing peak flame temperatures at lean overall equivalence ratios. Likewise, if the diluent is independently injected into the combustor as a separate stream, there are no guarantees that all of the diluent will arrive at the flame front to serve, essentially, as a heat sink. Thus, the use of the diluent for peak flame temperature suppression is maximized with the dilution of the fuel stream, regardless of whether or not swirl is utilized in the combustor.

However, from a flame front dilution perspective, this temperature effect diminishes with an increasing equivalence ratio. When a stoichiometric amount of air is supplied to the combustor, it is irrelevant whether the fuel or air is diluted, as all of the diluent must arrive at the flame front in either case. In traditional swirl-based diffusion flame combustors, the primary combustion zone typically operates at near-stoichiometric conditions, with the balance of the air used to provide liner cooling, complete CO burnout downstream, and create the desired pattern factor at the inlet to the turbine [21]. For these combustors, the effects of air- or fuel-side dilution have been found to be negligible due to the absence of a substantial flame temperature reduction [5,18], leading manufacturers to use air-side dilution for ease of implementation [17]. LDI combustors, on the other hand, strive to supply air at low equivalence ratios to the flame front for peak flame temperature NO_x reduction and rapid quenching of thermal NO_x reactions, thus fuel-side dilution is expected to achieve the maximum benefit in this regard.

It is important to note that this idealized flame temperature analysis does not account for other effects that often occur in actual combustor operations. For instance, if mixing times are relatively slow, the differential diffusion of hydrogen out of a hydrogen/nitrogen fuel jet may cause localized regions of higher hydrogen content and superequilibrium flame temperatures not accounted for in this analysis [28]. In addition, cases may arise in which independent diluent injection may be beneficial to LDI combustor operation, for instance, for cooling the injector surface

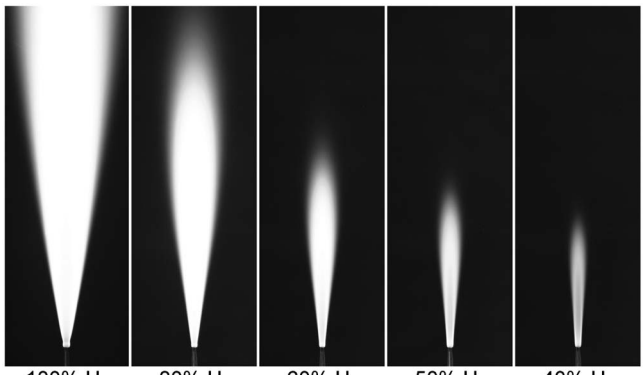

Fig. 3 Flame length versus the nitrogen dilution of hydrogen in a simple turbulent jet flame

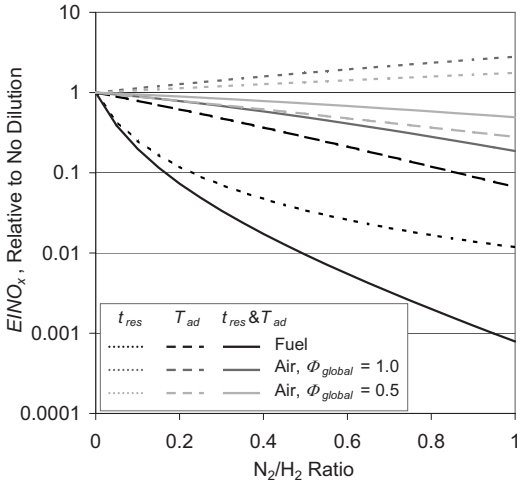

Fig. 4 Simple jet flame temperature and residence time scaling of NO_x emissions with air- and fuel-side dilutions

or for creating a nonreactive buffer zone that ensures that the flame does not attach to the injector and cause damage from overheating [13].

3.2 Flame Residence Time. The effect of air-side dilution versus fuel-side dilution on flame residence times and NO_x emissions is easily understood by considering the factors influencing the flame length of a simple momentum-dominated turbulent jet flame [29]

$$L_f \propto \frac{d_F}{f_s}\left(\frac{\rho_F}{\rho_A}\right)^{1/2} \tag{4}$$

where f_s is a stoichiometric mixture fraction and ρ_F and ρ_A are the fuel and air densities, respectively. This similarity-based scaling heavily influences the flame residence time through its cubic dependence on flame length. Under this scaling, the fuel jet's momentum increases linearly with its density, and the conservation of momentum requires that the mass entrainment of air increase in proportion, resulting in a velocity-independent flame length scaling. With the N_2 dilution of H_2 fuel, this yields increased turbulent mixing and more oxygen available for combustion of a smaller amount of fuel, by volume. The overall effect of decreasing the flame height by simultaneously increasing the jet density and stoichiometric mixture fraction through fuel-side dilution, according to Eq. (4), can be seen in Fig. 3. Note that the stoichiometric mixture fraction for a pure hydrogen fuel burning in ambient air is $f_s=0.03$. Adding an equal part of nitrogen by volume to the fuel stream ($N_2/H_2=1$) yields $f_s=0.30$, while adding this same quantity of nitrogen to a stoichiometric air stream instead yields $f_s=0.02$.

Chen and co-workers [26,30,31] have shown that for pure and diluted hydrogen jet flames, the NO_x emission index, normalized by the flame's characteristic residence time, is proportional to the square root of the global strain rate of the flame $(U_F/d_F)^{1/2}$. This gives rise to the $Da^{-1/2}$ scaling in Eq. (2) for a given fuel composition, and results from turbulence-chemistry interactions that arise at high mixing rates. Including the effect of global flame strain with residence time, the NO_x emission scaling of Eq. (2) for a simple turbulent jet flame, excluding temperature effects, can be expressed as

$$EINO_x \propto \frac{L_f^3}{U_F d_F^2}\left(\frac{U_F}{d_F}\right)^{1/2} \propto \frac{1}{f_s^3}\left(\frac{d_F}{U_F}\right)^{1/2}\left(\frac{\rho_F}{\rho_A}\right)^{3/2} \tag{5}$$

For a given fuel jet diameter and hydrogen flow rate, the scaling of Eq. (5), normalized by the case for no dilution, is plotted against the N_2/H_2 ratio in Fig. 4 for fuel- and air-side dilutions at two different global equivalence ratios (dotted lines). From a residence time perspective, Fig. 4 shows that the effect of air-side dilution is to increase NO_x emissions, primarily due to an increase in flame volume, while fuel-side dilution can reduce NO_x by two orders of magnitude in a simple jet flame. The effects of flame temperature on NO_x, as embodied in Eq. (3) and Fig. 2, are plotted as dashed lines in Fig. 4, where the effects of fuel-side dilution and air-side dilution at $\Phi_{global}=1$ are identical, as noted in Sec. 3.1. The solid lines in Fig. 4 show the combined effect of temperature, residence time, and global flame strain on NO_x, according to Eq. (2). For air-side dilution, the potential NO_x reductions due to flame temperature are tempered somewhat by the adverse residence time effect, while the combined temperature and residence time effects yield substantially higher NO_x reduction potential for fuel-side dilution.

While not likely to be directly applicable to many LDI injector designs, this analysis illustrates that residence time reduction is very important to decreasing NO_x emissions in LDI combustors. In addition, the dilution of the air or fuel streams can have a significant effect on the fuel/air mixing in cases where mass entrainment by a jet is relied upon to produce or enhance mixing. In particular, the dilution of a low-density hydrogen fuel jet, even with a small amount of premixed air, may drastically increase its jet momentum and mixing characteristics, which is an important consideration in LDI injector styles that rely on jet-in-crossflow configurations for mixing [12,13], and in swirl-based injectors in which a fuel jet penetrates into a swirling air flow [5–7].

Before leaving the topic of simple jet flames, it is important to note that many of the above results are specific to the use of hydrogen as a fuel, and will be altered by the presence of other fuel components such as CO or methane. In particular, the above results are primarily applicable to the thermal NO_x generation mechanism, and are further complicated by the inclusion of the prompt NO_x mechanism, which accompanies the use of hydrocarbons as fuel components [19,30].

3.3 Operating Regimes. Jet entrainment alone does not provide adequate fuel/air mixing to create a realistic jet-based LDI injector. Forced mixing strategies such as angled injection, in which fuel and air jets impinge upon one another, are frequently used to significantly reduce flame lengths, residence time, and hence NO_x emissions [13,14]. Since these geometry-dependent schemes do not lend themselves to parametric or analytical study, the current study utilizes the coaxial air injection scheme shown in Fig. 1 to simulate various aspects of the forced mixing strategy.

Analytically, the flame length of a staged coaxial air flame, as utilized in this study, can be expressed as [26,32]

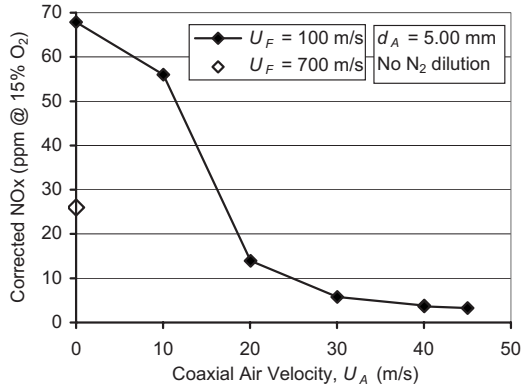

Fig. 5 NO_x reduction with increased mixing from coaxial air flow without dilution

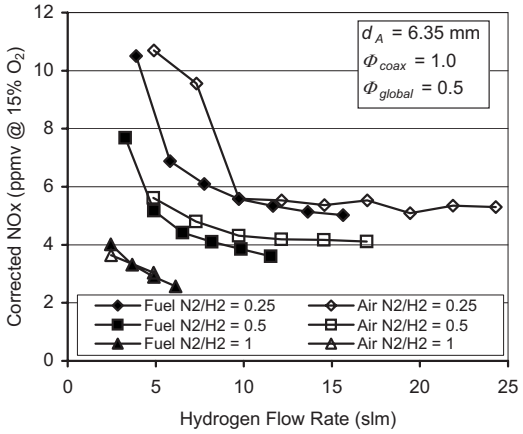

Fig. 6 Effect of air-side dilution versus fuel-side dilution on NO_x with d_A=6.35 mm and Φ_{coax}=1

$$L_f \propto \frac{d_F}{f_s}\sqrt{\frac{\rho_F/\rho_A}{1+\frac{\rho_A U_A^2(d_A^2-d_{F,o}^2)}{\rho_F U_F^2 d_F^2}}} \tag{6}$$

where U_A is the coaxial air velocity. This equation quantifies the effects of coaxial air jet momentum on reducing the overall flame length. Although this is a good indicator of reduced flame residence time, it should be noted that L_f^3 is no longer proportional to the flame volume for a coaxial air flame [33], thus the simple residence time scaling in Eq. (5) no longer applies.

The effect of coaxial air on NO_x emissions for a simple hydrogen/air flame with no nitrogen dilution can be seen clearly in Fig. 5. For a fuel jet velocity of 100 m/s with no coaxial air, a baseline reading of 68 ppm NO_x at 15% O_2 is attained. Increasing coaxial air to 45 m/s reduces the flame length considerably, resulting in about 3.3 ppm NO_x, though increasing the coaxial air velocity further results in blowoff. While a seemingly large reduction in NO_x is attained, note that the flame is very stable at U_F = 100 m/s without coaxial air, but is on the verge of blowoff with 45 m/s coaxial air, a substantial reduction in the flame's stability margin. A more reasonable comparison would consider the 45 m/s coaxial air case against a case with a similar stability margin, i.e., just before blowoff. Although the required fuel flow could not be attained for this case, in the absence of coaxial air flow the flame should detach from the burner at $U_F \approx 700$ m/s, yielding about 26 ppm NO_x at 15% O_2 according to the scaling of Eq. (5). The addition of high velocity coaxial air therefore represents a factor of 8 reduction in the NO_x output at a similar stability condition.

Maximizing the utilization of a diluent for peak flame temperature reduction purposes dictates that the diluent be added to the coaxial air flow, adjacent to the fuel jet, rather than the coflow air in the current configuration. In addition, if the coaxial air equivalence ratio is limited to $\Phi_{coax} > 1$, then coaxial air dilution could potentially reduce the flame temperature as well as fuel-side dilution. In this case, forced mixing ensures that nearly all of the coaxial air will be mixed with the hydrogen fuel jet prior to complete combustion, allowing the diluent to reduce combustion temperatures and thermal NO_x production at the flame front.

For the simple coaxial air arrangement discussed above, using d_A=6.35 mm, the effects of movement of the nitrogen diluent from the coaxial air stream to the hydrogen fuel stream on NO_x emissions are shown in Fig. 6. In these experiments, for a given hydrogen flow rate in standard L/min (slm), a stoichiometric amount of air is supplied through the coaxial air flow (Φ_{coax} =1.0), with the same amount of air also supplied via the low-velocity coflow air. This arrangement yields a constant global equivalence ratio (Φ_{global}=0.5) and provides a direct comparison between nitrogen diluent placement in either the air or fuel streams, accounting for differences in the air and fuel velocities caused by the diluent. Figure 6 reveals that at most, 10% reduction in NO_x is achieved in this case by diluting the hydrogen stream rather than the air stream. In addition, note that in the case of low nitrogen dilution, higher hydrogen flow rates are attained for coaxial air dilution than for fuel dilution, while the opposite is true at high nitrogen dilution levels.

As with the diluent-free case in Fig. 5, it is worthwhile to consider the effect of dilution on combustor stability margins, where the potential to reduce NO_x emissions via residence time reductions can result from high velocity fuel and air injections. The practical stability limits of coaxial air flames are linked to the flameholding mechanism, in which the flame attaches to the fuel tube in the low-velocity wake region behind the fuel tube's lip thickness. This wake region extends from the edges of the tube lip up to the intersection of the jet's shear layers, and contains a potentially combustible mixture of fuel and air. Similar flameholding regions exist in jet-type LDI injectors [13,14], though angled fuel or air injection may create stronger recirculation vortices within this wake region.

For coaxial air flames attached to the tube lip, instability can occur in one of two primary ways [34]: detachment of the flame base from the wake region, sometimes leading to the formation of a lifted flame, and the creation of a "split flame" as shown in Fig. 7(*c*), where high shear strain creates a region of local flame extinction at the intersection of the jet shear layers. In a split flame, a "rim flame" exists within the wake region of the fuel tube, and supplies heat and radicals to the upper flame above the shear layer

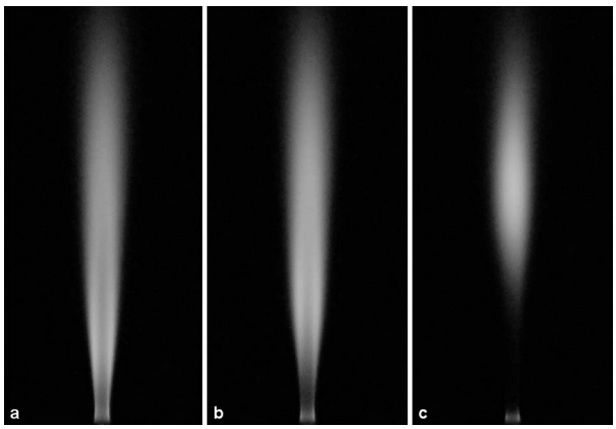

Fig. 7 Split flame formation for d_A=5.00 mm, N_2/H_2=0.25, and Φ_{coax}=0.5. (*a*) Stable flame at U_F=100 m/s, (*b*) near split flame at 120 m/s, and (*c*) split flame at 140 m/s

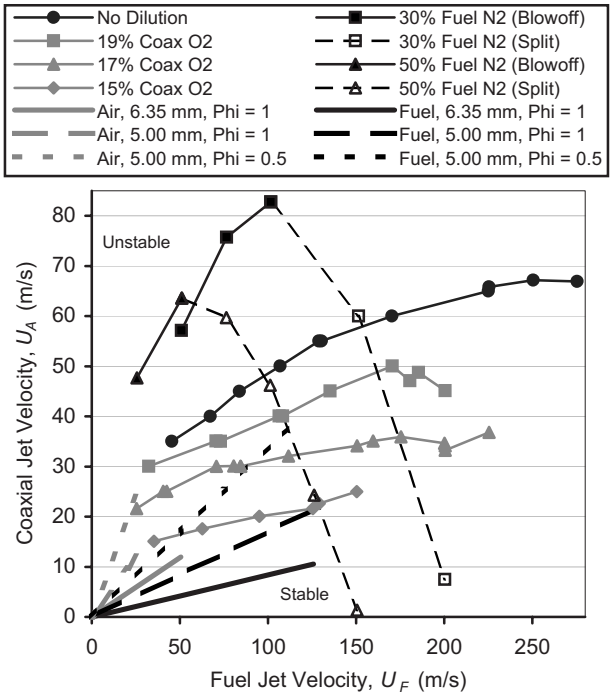

Fig. 8 Stability regimes for coaxial air-side dilution versus fuel-side dilution using d_A=5.00 mm. Air dilution is expressed in terms of the resulting percent oxygen in the air. NO_x test conditions of Fig. 9 for N_2/H_2=1 are shown as lines of constant U_F/U_A emanating from the origin.

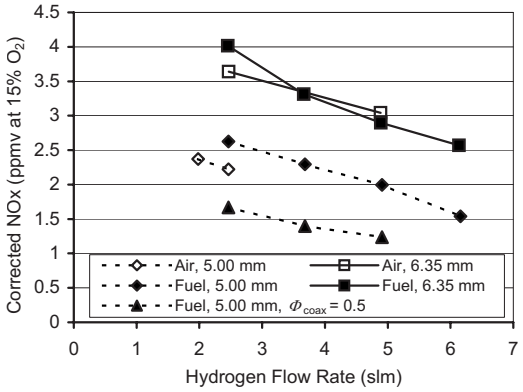

Fig. 9 Corrected NO_x measurements for N_2/H_2=1, as a function of diluent placement, d_A, and Φ_{coax} (=1 unless otherwise noted)

intersection. In very high coaxial air flows, the upper flame can be extinguished altogether, leaving a residual rim flame at the injector tip [35]. Stability limits relating to the formation of a split coaxial air flame are applicable, to some extent, to the high strain regions at the point of jet impingement in an angled injection LDI burner.

Stability limits for air- and fuel-side dilutions are shown in Fig. 8 as a function of jet exit velocities for the d_A=5.00 mm coaxial air case. For the dilute fuel cases, the "blowoff" results indicate conditions in which a rim-attached flame abruptly blows off the burner without establishing a stable lifted flame, while the "split" limits correspond to the point at which the tip of the split flame extinguishes, leaving a residual rim flame attached to the fuel tube (i.e., very low combustion efficiency). For the dilute coaxial air cases, the nitrogen diluent is expressed in terms of the resulting oxygen content of the coaxial air stream. For reference, the N_2/H_2=0.25, Φ_{coax}=1 and N_2/H_2=0.5, Φ_{coax}=0.5 cases both result in 19.0% O_2 content; the N_2/H_2=0.5, Φ_{coax}=1 and N_2/H_2=1, Φ_{coax}=0.5 cases both result in 17.4% O_2 content; and the N_2/H_2=1, Φ_{coax}=1 case yields 14.8% O_2 content in the coaxial air stream. In these cases, only the blowoff stability limit is shown, although the maximum hydrogen jet velocities plotted are those at which a stable jet flame exists. Higher fuel jet velocities can result in lifted or split flames, as discussed above, although lifted flames were not observed for the dilute fuel cases in this study.

The results of Fig. 8 show that for the increasing nitrogen dilution of the coaxial air, both the maximum stable fuel jet and coaxial air velocities decrease. The stability limit governing the formation of a split flame seems to be equally affected by air or fuel dilution, as decreasing fuel jet velocities are accompanied by the dilution of either stream. This is consistent with a decrease in flame speed and/or flame temperature in the high strain regions characterized by fast mixing rates, in which nitrogen diluent is present regardless of its point of origin.

The most interesting result from Fig. 8 is that the addition of nitrogen to the fuel jet increases the attainable air/fuel velocity ratio, even above the case in which there is no diluent present. For instance, 70 m/s or 80 m/s coaxial air is not attainable for a pure H_2 jet, but can be attained with 30% N_2 dilution in the hydrogen. This is related to the entrainment properties of the fuel jet and its effect on the fuel/air stoichiometry in the wake region, as will be discussed in Sec. 3.4.

Although not shown here, it should be noted that, from a jet velocity perspective, the stability regimes of Fig. 8 are not a function of the coaxial air jet diameter. In addition, the stability limits can be further increased by increasing the fuel tube lip thickness, though there is an upper limit beyond which increasing lip thickness ceases to increase the stability limit [35], which is related to the quenching distance for a given fuel/air mixture [34]. Furthermore, decreasing the fuel jet diameter serves to increase the stability limits as well [35], which also reduces NO_x emissions through reduced flame residence times.

The resulting effect of the dilution placement on the combustor's stability margins is shown in Fig. 8 for N_2/H_2=1, where moving the nitrogen diluent from the coaxial air to the fuel side results in increases in attainable fuel and air velocities, as determined by their respective stability regimes. These increases in fuel and air velocities for fuel dilution can be expected to yield a decrease in residence time and NO_x emissions according to Eqs. (5) and (6).

Measured NO_x reductions for these N_2/H_2=1 cases are illustrated in Fig. 9, where replacing the 6.35 mm diameter coaxial air nozzle with the 5.00 mm nozzle has the effect of doubling the coaxial air velocity at a given volume flow rate (or Φ_{coax}) of coaxial air. This results in a 30–40% reduction in NO_x at a given hydrogen flow rate, as shown in Fig. 9, although increased stability margins allow for much higher hydrogen flow rates, and hence lower NO_x, for fuel-side dilution with the 5.00 mm coaxial air jet diameter. To further illustrate this benefit, the dilute fuel case in which all of the air is supplied through the coaxial air jet (Φ_{coax}=0.5) is also shown, where doubling the air velocity again further reduces NO_x by about 38%. Turbulent flames are not attainable at these hydrogen flow rates and coaxial air velocity levels using air-side dilution, as the blowoff stability limit is exceeded, as shown in Fig. 8. Thus, the operating regimes attainable with fuel-side dilution allow for greater NO_x reduction than those attainable with air-side dilution in the coaxial air configuration. Similar results should be expected for angled LDI-injection schemes, as the stability mechanisms that determine the operating regimes of these burners are similar to those of the current study.

3.4 Flameholding Mechanism. The predominant stability mechanism that is relevant to coaxial air and angled LDI-injection burners is blowoff of the rim flame from the small recirculation

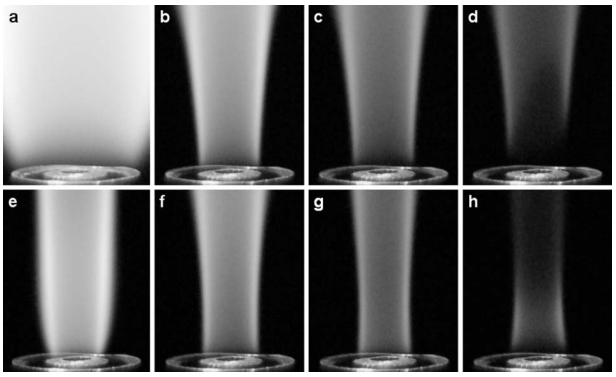

Fig. 10 Flame base photos with U_F=75 m/s and d_A =5.00 mm: (*a*) U_A=0 m/s, no dilution; (*b*) U_A=15 m/s, no dilution; (*c*) U_A=15 m/s, 17.4% coaxial air O_2; (*d*) U_A=15 m/s, 14.8% coaxial air O_2; (*e*) U_A=0 m/s, fuel N_2/H_2=1; (*f*) U_A =15 m/s, fuel N_2/H_2=0.5; (*g*) U_A=15 m/s, fuel N_2/H_2=1; and (*h*) U_A=45 m/s, fuel N_2/H_2=1

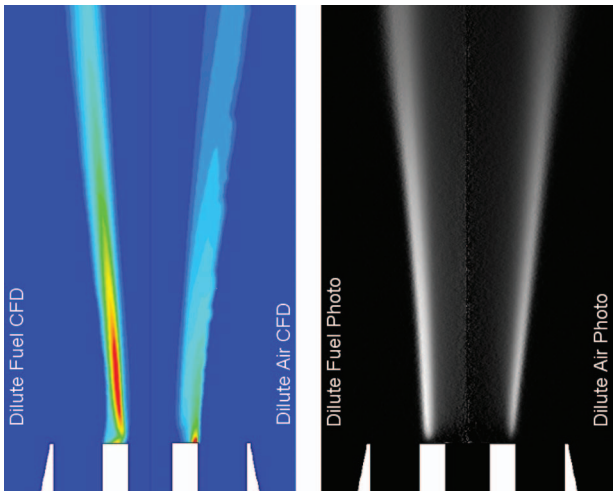

Fig. 11 Comparison of CFD H_2O formation rate with flame luminosity for fuel and air dilutions using d_A=6.35 mm, 5 slm H_2, N_2/H_2=0.5, and Φ_{coax}=1, up to x/d_F=10

region between the fuel and air injection points. This region is typically small enough that heat transferred from the attached flame to the burner surface can be sufficiently removed by the incoming fuel and air flows to prevent thermal damage to the burner. As discussed above in connection with Fig. 8, the blowoff velocity associated with the flameholding mechanism in this region is significantly increased with fuel-side dilution and reduced with air-side dilution. This leads to increased flameholding ability in the recirculation region with fuel-side dilution, while air-side dilution can be used in cases where flameholding on the LDI injector face is to be avoided to reduce the risk of overheating, provided that another stability mechanism is employed to anchor the flame in this situation.

The flameholding mechanism is primarily a function of the stoichiometry in the recirculation region, which is a balance between hydrogen diffusion out of the fuel jet and radial air velocity toward the fuel jet. In the absence of a coaxial air flow, the diffusion of hydrogen out of the fuel jet is such that the flame base is established far outside the jet's shear layer, as shown in Fig. 10(*a*). With the addition of a small amount of coaxial air, the flame stabilization point moves to the outer edge of the fuel tube as shown in Fig. 10(*b*). Adding nitrogen diluent to the coaxial air reduces the flame temperature and reaction rate at this location, due to reduced oxygen availability, eventually leading to extinction of the flame when the reduced temperature and radical production rate can no longer sustain the flame. This is shown in Figs. 10(*c*) and 10(*d*), where the visible luminosity of the anchored flame, primarily the result of H_2O thermal broadband emissions [36], diminishes with increasing coaxial air nitrogen content. By contrast, the dilution of the fuel stream has a reduced impact on the stability of the rim flame (comparing Fig. 10(*c*) to Fig. 10(*f*), and Fig. 10(*d*) to Fig. 10(*g*)). In this case, hydrogen diffuses across the wake region much more quickly than nitrogen, minimizing the concentration of the diluent nitrogen at the location of the flame base near the fuel tube's outer rim, and increasing its stability characteristics.

With the increasing nitrogen dilution of the fuel, the rate of the differential diffusion of hydrogen out of the fuel jet decreases due to a decrease in the species concentration gradient across the wake region. In addition, the momentum of the fuel jet increases with increasing jet density (via dilution) and/or jet velocity, thus increasing its mass entrainment requirements and hence the radial inflow of air toward the fuel jet. Eventually, the inward air velocity exceeds the outward hydrogen diffusion velocity, moving the flame base toward a more stable location closer to the fuel jet (Figs. 10(*b*), 10(*f*), and 10(*g*)), thereby enhancing flame stability with fuel jet dilution as seen in Fig. 8. Increasing the dilute fuel jet velocity leads to the formation of an inefficient split flame well before extinction of the rim flame, while increasing the coaxial air velocity eventually leads to lifting of the rim flame off of the fuel tube (Fig. 10(*h*)) and extinction as the flame base approaches the high strain region at the intersection of the jet shear layers.

The various nuances of the rim flame stability mechanism in coaxial air flames are also important in angled LDI-injection schemes. CFD is a valuable tool for assessing the feasibility of these angled injection schemes without resorting to parametric experimental studies of the multitude of possible geometric configurations (injection angles, hole sizes, hole spacing, and so on). Accurately modeling the flowfield and differential diffusion characteristics in the flameholding recirculation region between the fuel and air injection points is essential to the success of such CFD models, and it can be verified with the simplified coaxial air mechanism employed in this study. Attaining a stable, anchored flame in CFD models of the coaxial air configuration requires the use of a turbulence-chemistry interaction model that models the differential diffusion process accurately. While probability distributio function models do not account for such processes, the EDC model does allow for differential diffusion [24]. Several 2D, axisymmetric CFD simulations were conducted using the FLUENT code, using a Reynolds stress turbulence model, the EDC combustion model and the H_2/O_2 mechanism of Li et al. [25]. The 35,000 cell computational domain encompassed the entire experimental apparatus including the fuel and air inlets and passageways and the full combustor can downstream to the exit. The inlets were prescribed as mass flow inlets and the exit of the combustor as a pressure outlet boundary. The walls of the combustor were set at a fixed temperature of 500 K, which was approximately equal to the average surface temperature measured in the experiments. Stable flame models could typically only be attained by first specifying a high-temperature condition (1500 K) at the fuel tube tip to maintain flame stability until some degree of convergence was attained with the initial velocity and species fields, after which this temperature boundary condition was replaced by an adiabatic boundary condition.

Figure 11 compares the CFD modeling results for fuel- and air-side dilution cases with near-field photos taken under the same conditions at a spatial resolution of 26.5 μm and an exposure time of 5 s. Radius-dependent line-of-sight averaging effects are removed from the flame photos by using an Abel inversion routine [37], and the contrast is enhanced to yield the radial flame profiles shown on the right side of Fig. 11. The modeled H_2O formation rate matches well with the luminous flame photo locations and

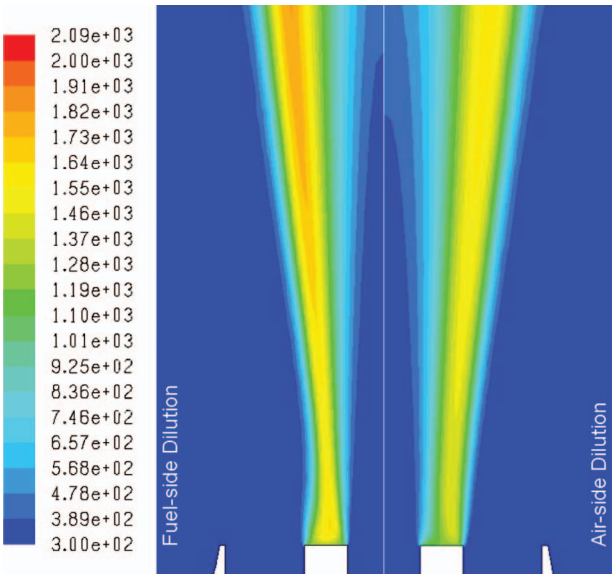

Fig. 12 Computed near-field flame temperatures. Same conditions as in Fig. 11.

intensities, as expected. The effects of air-side dilution versus fuel-side dilution also match observations fairly well, showing their respective flame base locations at the outer edge of the fuel tube rim and center of the fuel tube rim.

The details of the flame base location are also evident in Fig. 12, which shows the enhanced stability of the fuel-side dilution case in the increased flame temperature within the recirculation region. Differential diffusion effects resulting from fuel-side dilution can also be seen in the downstream portions of this figure, where higher hydrogen content causes increased flame temperatures compared with the dilute coaxial air case. Furthermore, the air flow and differential diffusion effects on flame stability can also be seen in Fig. 13, where a line denoting stoichiometric conditions ($H_2/O_2=2$) is superimposed on the velocity field in the recirculation region. This figure reveals that the net radial velocity in the recirculation region is toward the jet with the higher velocity (i.e., the fuel jet), as determined previously by water-table [35] and laser Doppler velocimetry [34] experiments. In addition, the high-hydrogen content at the outer edge of the fuel tube in the air-dilution case is indicative of a high rate of hydrogen diffusion radially out of the fuel jet, in spite of a radial inflow of air. The dilute fuel case, meanwhile, shows that the increased inward air velocity shifts the stoichiometric H_2/O_2 mixture toward the fuel jet.

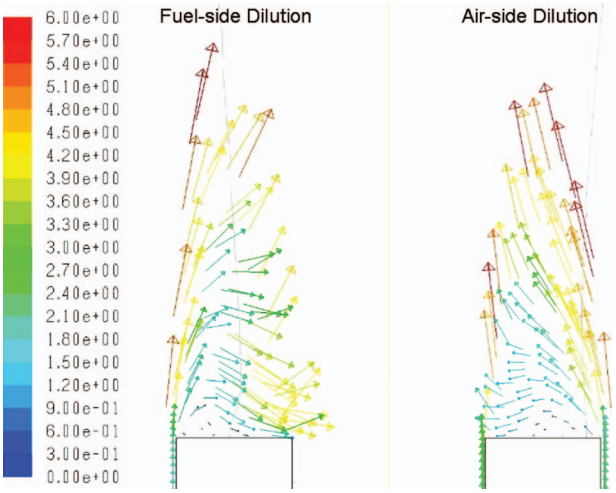

Fig. 13 Computed velocity vectors (max 6 m/s shown) and stoichiometric location in the wake region of the fuel tube. Same conditions as in Fig. 11.

4 Conclusions

The use of a nitrogen diluent in either the fuel or air streams of an LDI-style combustor has been investigated from several viewpoints, for the overall purpose of reducing NO_x emissions. The use of the diluent for reducing the peak flame temperature, and hence the NO_x emissions, is maximized with fuel stream dilution, as all of the nitrogen must pass through the flame front along with the fuel. Likewise, fuel-side dilution also minimizes the flame residence time in a simple turbulent jet diffusion flame, thus reducing NO_x emission. Although this is an unrealistic approximation of an LDI-style injector, the analysis illustrates the effects of dilution on fuel/air mixing processes, particularly the effect of nitrogen dilution on the hydrogen jet momentum and penetration, which applies in both swirl-based and jet-based LDI-injection schemes. For jet-based LDI burners, flame stability issues within the recirculation region between the fuel and air injection points, and at the intersection between their respective shear layers, plays an important role in determining the operating regimes that are attainable with either air- or fuel-side dilution. For the coaxial air flame considered in this study, the dilution of the fuel stream was preferable in that it allowed for higher fuel and air velocities to be attained, which serve to further reduce flame residence times and NO_x emissions. This is largely due to differential diffusion of hydrogen out of the hydrogen/nitrogen fuel jet, leading to the formation of a very stable, mostly diluent-free flame base in the recirculation region between the fuel and air jets. Properly modeling this flame anchoring behavior is essential to the success of CFD codes for investigating more complex angled injection LDI schemes, and it has been performed with reasonable success using the modeling technique in the current study.

Acknowledgment

The support from the Turbines Program of the U.S. Department of Energy is gratefully acknowledged, along with the administrative support of the Oak Ridge Institute for Science and Education. A portion of this technical effort was performed in support of the National Energy Technology Laboratory's ongoing research in hydrogen gas turbine combustion under the RDS Contract No. DE-AC26-04NT41817.

Nomenclature

D = moles of nitrogen diluent per mole of hydrogen
Da = Damköhler number
d_A = coaxial air nozzle inside diameter
d_F = fuel tube inside diameter
$d_{F,o}$ = fuel tube outside diameter
$EINO_x$ = NO_x emission index (g NO_2/kg H_2)
f_s = stoichiometric mixture fraction
L_f = flame length
T = flame temperature (K)
T_{ad} = adiabatic flame temperature (K)
t_{res} = flame residence time
U_A = coaxial air exit velocity
U_F = fuel jet exit velocity
$\chi_{NO_x,meas}$ = measured NO_x (ppm)
$\chi_{NO_x,corr}$ = corrected NO_x (ppm)
$\chi_{O_2,meas}$ = measured product gas O_2 mole fraction
Φ_{coax} = coaxial air equivalence ratio
Φ_{global} = global equivalence ratio
ρ_A = air density

ρ_F = fuel density
$[X]$ = molar concentration of species X

References

[1] Vogt, R. L., 1980, "Low Btu Coal Gas Combustion in High Temperature Turbines," ASME Paper No. 80-GT-170.
[2] Beebe, K. W. and Blanton, J. C., 1985, "Design and Development of a Heavy-Duty Industrial Gas Turbine Combustion System for Low-Btu Coal Gas Fuel," ASME Paper No. 85-GT-45.
[3] Becker, B., and Schetter, B., 1993, "Use of LHV Gas in a Gas Turbine," Bioresour. Technol., **46**, pp. 55–64.
[4] Kelsall, G. J., Smith, M. A., and Cannon, M. F., 1994, "Low Emission Combustor Development for an Industrial Gas Turbine to Utilize LCV Fuel Gas," ASME J. Eng. Gas Turbines Power, **116**, pp. 559–566.
[5] Battista, R. A., and Dudley, J. C., 1995, "Full-Scale F Technology Combustor Testing of Simulated Coal Gas," DOE Final Report No. DOE-MC/27221-1.
[6] Reiss, F., Griffin, T., and Reyser, K., 2002, "The Alstom GT13E2 Medium BTU Gas Turbine," ASME Paper No. GT-2002-30108.
[7] Ziemann, J., Shum, F., Moore, M., Kluyskens, D., Thomaier, D., Zarzalis, N., and Eberius, H., 1998, "Low-NO_x Combustors for Hydrogen Fueled Aero Engine," Int. J. Hydrogen Energy, **23**(4), pp. 281–288.
[8] Tacina, R. R., Wey, C., and Choi, K. J., 2001, "Flame Tube NO_x Emissions Using a Lean-Direct-Wall-Injection Combustor Concept," Paper No. AIAA-2001-3271.
[9] Tacina, R., Wey, C., Liang, P., and Mansour, A., 2002, "A Low NO_x Lean-Direct Injection, Multipoint Integrated Module Combustor Concept for Advanced Aircraft Gas Turbines," NASA Report No. TM-2002-211347.
[10] Hernandez, S. R., Wang, Q., McDonell, V., Mansour, A., Steinthorsson, E, and Hollon, B., 2008, "Micro-Mixing Fuel Injectors for Low Emissions Hydrogen Combustion," ASME Paper No. GT2008-50854.
[11] Hernandez, S., Wang, Q., Lee, H., McDonell, V., Hollon, B., Mansour, A., and Steinthorsson, E., 2008, "Micro-Mixing Fuel Injection for Low Emission Combustion of Hydrogen for Gas Turbine Applications," International Pittsburgh Coal Conference, Pittsburgh, PA.
[12] Dahl, G., and Suttrop, F., 1998, "Engine Control and Low-NO_x Combustion for Hydrogen Fuelled Aircraft Gas Turbines," Int. J. Hydrogen Energy, **23**(8), pp. 695–704.
[13] Marek, C. J., Smith, T. D., and Kundu, K., 2005, "Low Emission Hydrogen Combustors for Gas Turbines Using Lean Direct Injection," Paper No. AIAA-2005-3776.
[14] GE Energy, 2005, "Premixer Design for High Hydrogen Fuels—Final Report," DOE Cooperative Agreement No. DE-FC26-03NT41893.
[15] Todd, D. M., and Battista, R. A., 2000, "Demonstrated Applicability of Hydrogen Fuel for Gas Turbines," *Proceedings of the IChemE "Gasification 4 the Future" Conference*, Noordwijk, The Netherlands.
[16] Chiesa, P., Lozza, G., and Mazzocchi, L., 2005, "Using Hydrogen as Gas Turbine Fuel," ASME J. Eng. Gas Turbines Power, **127**, pp. 73–80.
[17] Todd, D. M., 2000, "Gas Turbine Improvements Enhance IGCC Viability," Gasification Technologies Conference, San Francisco, CA.
[18] Cook, C. S., Corman, J. C., and Todd, D. M., 1995, "System Evaluation and LBTU Fuel Combustion Studies for IGCC Power Generation," ASME J. Eng. Gas Turbines Power, **117**, pp. 673–677.
[19] Rokke, P. E., and Hustad, J. E., 2005, "Exhaust Gas Recirculation in Gas Turbines for Reduction of CO_2 Emissions; Combustion Testing With Focus on Stability and Emissions," Int. J. Thermodyn., **8**, pp. 167–173.
[20] Feese, J. J., and Turns, S. R., 1998, "Nitric Oxide Emissions From Laminar Diffusion Flames: Effect of Air-Side Versus Fuel-Side Diluent Addition," Combust. Flame, **113**, pp. 66–78.
[21] Lefebvre, A. H., 1999, *Gas Turbine Combustion*, 2nd ed., Taylor and Francis, Ann Arbor.
[22] ElKady, A. M., Evulet, A., Brand, A., Ursin, T. P., and Lynghjem, A., 2008, "Exhaust Gas Recirculation in DLN F-Class Gas Turbines for Post-Combustion CO_2 Capture," ASME Paper No. GT2008-51152.
[23] Morley, C., 2005, "GASEQ: Chemical Equilibria in Perfect Gases," Version 0.79, http://www.gaseq.co.uk
[24] Magnussen, B. F., 1981, "On the Structure of Turbulence and a Generalized Eddy Dissipation Concept for Chemical Reaction in Turbulent Flow," Paper No. AIAA-1981-42.
[25] Li, J., Zhao, Z., Kazakov, K., and Dryer, F., 2004, "An Updated Comprehensive Kinetic Model of Hydrogen Combustion," Int. J. Chem. Kinet., **36**(10), pp. 566–575.
[26] Chen, R.-H., and Driscoll, J. F., 1990, "Nitric Oxide Levels of Jet Diffusion Flames: Effects of Coaxial Air and Other Mixing Parameters," Proc. Combust. Inst., **23**, pp. 281–288.
[27] Turns, S. R., 1995, "Understanding NO_x Formation in Nonpremixed Flames: Experiments and Modeling," Prog. Energy Combust. Sci., **21**, pp. 361–385.
[28] Meier, W., Prucker, S., Cao, M.-H., and Stricker, W., 1996, "Characterization of Turbulent H_2/N_2/Air Jet Diffusion Flames by Single-Pulse Spontaneous Raman Scattering," Combust. Sci. Technol., **118**, pp. 293–312.
[29] Delichatsios, M. A., 1993, "Transition From Momentum to Buoyancy-Controlled Turbulent Jet Diffusion Flames and Flame Height Relationships," Combust. Flame, **92**, pp. 349–364.
[30] Driscoll, J. F., Chen, R.-H., and Yoon, Y., 1992, "Nitric Oxide Levels of Turbulent Jet Diffusion Flames: Effects of Residence Time and Damköhler Number," Combust. Flame, **88**, pp. 37–49.
[31] Gabriel, R., Navedo, J. E., and Chen, R.-H., 2000, "Effects of Fuel Lewis Number on Nitric Oxide Emissions of Diluted H_2 Turbulent Jet Diffusion Flames," Combust. Flame, **121**, pp. 525–534.
[32] Dahm, W. J. A., and Mayman, A. G., 1990, "Blowout Limits of Turbulent Jet Diffusion Flames for Arbitrary Source Conditions," AIAA J., **28**(7), pp. 1157–1162.
[33] Chen, J.-Y., and Kollmann, W., 1992, "PDF Modeling and Analysis of Thermal NO Formation in Turbulent Nonpremixed Hydrogen-Air Jet Flames," Combust. Flame, **88**, pp. 397–412.
[34] Takahashi, F., and Schmoll, W. J., 1990, "Lifting Criteria of Jet Diffusion Flames," Sym. (Int.) Combust., [Proc.], **23**, pp. 677–683.
[35] Vranos, A., Taback, E. D., and Shipman, C. W., 1968, "An Experimental Study of the Stability of Hydrogen-Air Diffusion Flames," Combust. Flame, **12**, pp. 253–260.
[36] Halls, D. J., and Pungor, E., 1969, "An Examination of the Equilibrium Between H and OH Radicals and of Related Effects in Turbulent Hydrogen Flames as Used in Spectrophotometric Methods of Analysis," Anal. Chim. Acta, **44**, pp. 40–50.
[37] Villarreal, R., and Varghese, P. L., 2005, "Frequency-Resolved Absorption Tomography With Tunable Diode Lasers," Appl. Opt., **44**(31), pp. 6786–6795.